

Cite this: *Org. Biomol. Chem.*, 2023, **21**, 525

Received 10th November 2022,  
Accepted 12th December 2022

DOI: 10.1039/d2ob02061k

rsc.li/obc

## Introduction

The recognition of polar molecules in aqueous media stands as one of the major challenges in modern supramolecular chemistry.<sup>1</sup> Water is the biological solvent, thus the relevant medium for most biological applications. However, it presents special difficulties because of the competition of water for binding functionality in host and guest, while also providing the opportunity of hydrophobic interactions. Binding sites must be carefully designed to match polar groups in target substrates, *e.g.* with complementary hydrogen bonding units, while exploiting hydrophobic effects where possible. Solubility is also an issue; ideally, receptors should not only be water-soluble but monomeric at NMR concentrations, or they are difficult to study in full detail. Research activity is increasing, but there are still relatively few systems where polar and apolar interactions combine to achieve recognition in water.<sup>2</sup>

We have explored the “Temple” receptor architecture, in which hydrophobic aromatic roof and floor units are separated by polar spacers (pillars) (Fig. 1a).<sup>3</sup> The Temple layout is complementary to disc-like substrates with radially divergent polar groups and hydrophobic lower and upper surfaces, such as all-equatorial pyranoses ( $\beta$ -glucose and close relatives) and polar aromatics. The first-generation Temples employed isophthaloyl spacers furnished with dendrimeric polyanionic side chains to maintain water-solubility,<sup>4</sup> as exemplified in Fig. 1b. These macrocycles were moderately effective at binding carbo-

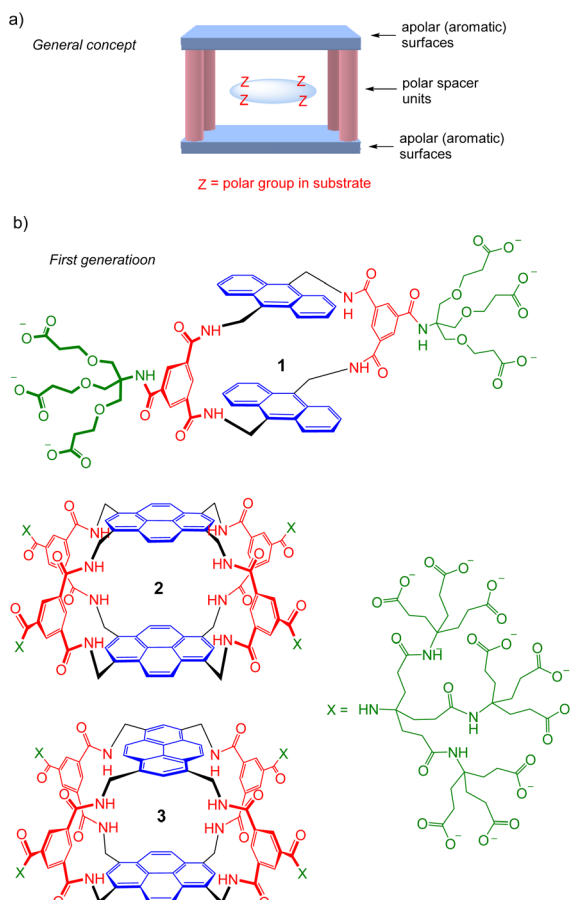


Fig. 1 (a) Schematic representation of the “Temple” receptor concept. (b) First-generation Temples with isophthaloyl spacers. Three examples are shown<sup>4d,e</sup> out of >20 published.

University of Bristol, School of Chemistry, Cantock's Close, Bristol, BS8 1TS, UK.

E-mail: anthony.davis@bristol.ac.uk

† Electronic supplementary information (ESI) available. See DOI: <https://doi.org/10.1039/d2ob02061k>



hydrates, which were our main objective and are intrinsically very challenging substrates.<sup>3</sup> For example, monocycle **1** bound glucose in water with  $K_a \sim 60 \text{ M}^{-1}$  (ref. 4d) while tricycles **2** and **3** achieved  $120 \text{ M}^{-1}$  and  $190 \text{ M}^{-1}$  respectively.<sup>4e</sup> Unfortunately for our carbohydrate-binding programme, they were also effective for polar aromatic substrates, where some very high affinities were measured (e.g.  $\sim 10^7 \text{ M}^{-1}$  for the biogenic heterocycle hypoxanthine).<sup>5</sup> Biological media contain various polar aromatics, circumscribing potential applications as “synthetic lectins”.<sup>3a</sup>

Seeking to tune the system in favour of carbohydrates, we then embarked on a second generation of Temples in which the spacer incorporates two urea groups and is one bond longer than the first-generation isophthalamide unit (Fig. 2). Prototype **4** was synthesised and tested as a receptor for glucose, and was outstandingly successful. Termed “GluHUT” (Glucose-Binding Hexaurea Temple), receptor **4** bound glucose with  $K_a \sim 20\,000 \text{ M}^{-1}$ , excellent selectivity over other carbohydrates and no detectable binding to non-carbohydrate substrates including polar aromatic compounds.<sup>6</sup>

Following the success of GluHUT **4**, we are interested in exploring the properties of other second-generation Temples featuring the new bis-urea spacers. Pyrene-based tricycles **2** and **3** had proved very effective in the earlier, first-generation series,<sup>4e</sup> so we concluded that the second-generation analogues **5** and **6** should be worth investigating. Here we report the syn-

thesis of tricyclic octaureas **5** and **6**, and studies of their binding properties towards carbohydrates and certain polar aromatics. The results suggest that these tricycles do not maintain open cavities in aqueous media, and do not bind carbohydrates as a consequence. However, the cavities can open to accept some substrates, with major changes in fluorescence output. As a result, these tricyclic octaureas are effective receptors/sensors for methylated purine alkaloids such as caffeine. They also bind very strongly to certain designed substrates, pointing to applications in supramolecular self-assembly.

## Results and discussion

### Synthesis

The two receptors were prepared in organic-soluble, *t*-butyl protected form as summarised in Scheme 1. The conversion of pyrene **7** into tetra-azide **8** was accomplished as described previously for the synthesis of **2** and **3**.<sup>4e</sup> The sequence is designed to bypass solubility problems, a key issue in pyrene chemistry. Solubility was again an issue in the further conversion of **8** to tetraisocyanate **9**; for example, the tetra-amine resulting from the reduction of **8** was insoluble in all organic solvents tested. Fortunately, the direct conversion of **8** to **9** via aza-Wittig<sup>7</sup> reaction with  $\text{CO}_2$  proved workable and highly efficient. Nearly quantitative yields of pure **9** could be obtained if high pressures ( $\sim 20$  bar) of  $\text{CO}_2$  were used with polymer-supported triphenylphosphine.<sup>8</sup> The tetra-isocyanate was combined with protected diamine **10**<sup>6</sup> to give “half-receptor” **11**, which was then cyclised with **9** to give organic-soluble cages **12** and **13**, separable by HPLC, in a ratio of  $\sim 2 : 1$ . Treatment of each with trifluoroacetic acid (TFA) to remove the *t*-butyl groups, followed by suspension in water and neutralisation to  $\text{pH} = 7.4$  with NaOH, led to the water-soluble cages **5** and **6**. Distinguishing between the two isomers was not immediately feasible, but could be achieved in the context of binding studies (see later).

### Conformational and binding studies

Receptors **5** and **6** were initially characterised by NMR and optical spectroscopy. The  $^1\text{H}$  NMR spectra of both receptors in  $\text{D}_2\text{O}$  were severely broadened at  $25^\circ\text{C}$  but sharpened appreciably as the temperature was raised to  $85^\circ\text{C}$ . Dilution studies on both receptors, covering the range  $750\text{--}63 \mu\text{M}$ , yielded no signal movements in either case suggesting that the broad spectra were due to conformational equilibria rather than aggregation. UV-Visible absorption spectra revealed bands at 330, 350 and 370 nm as expected for pyrene units, and fluorescence spectroscopy gave weak bands at 385 and 405 nm as well as a much larger, structureless emission between 430 and 580 nm for both receptors (Fig. 3). The bands at 385 and 405 nm are consistent with emission of pyrene monomer, while the broad emission at 430–580 nm implies the formation of the pyrene excimers, which can occur when two pyrene molecules are in close proximity to each other.<sup>9,10</sup> Notably, excimer formation was not observed for receptors **2** and **3**,<sup>4e</sup> despite the fact that the isophthaloyl linker is a bond shorter

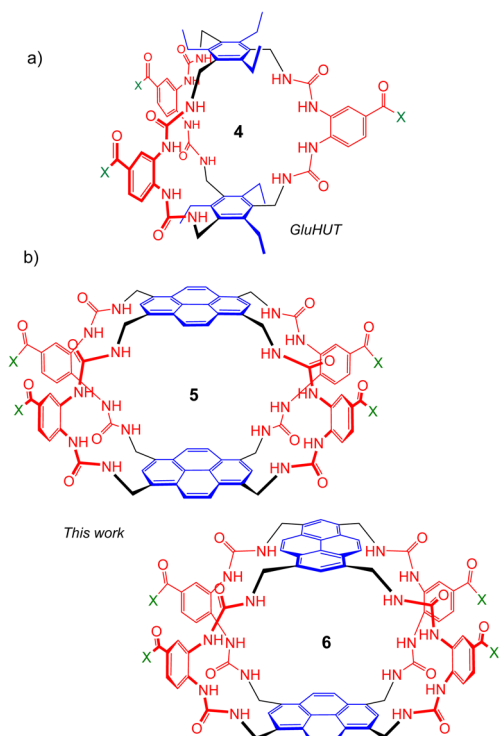
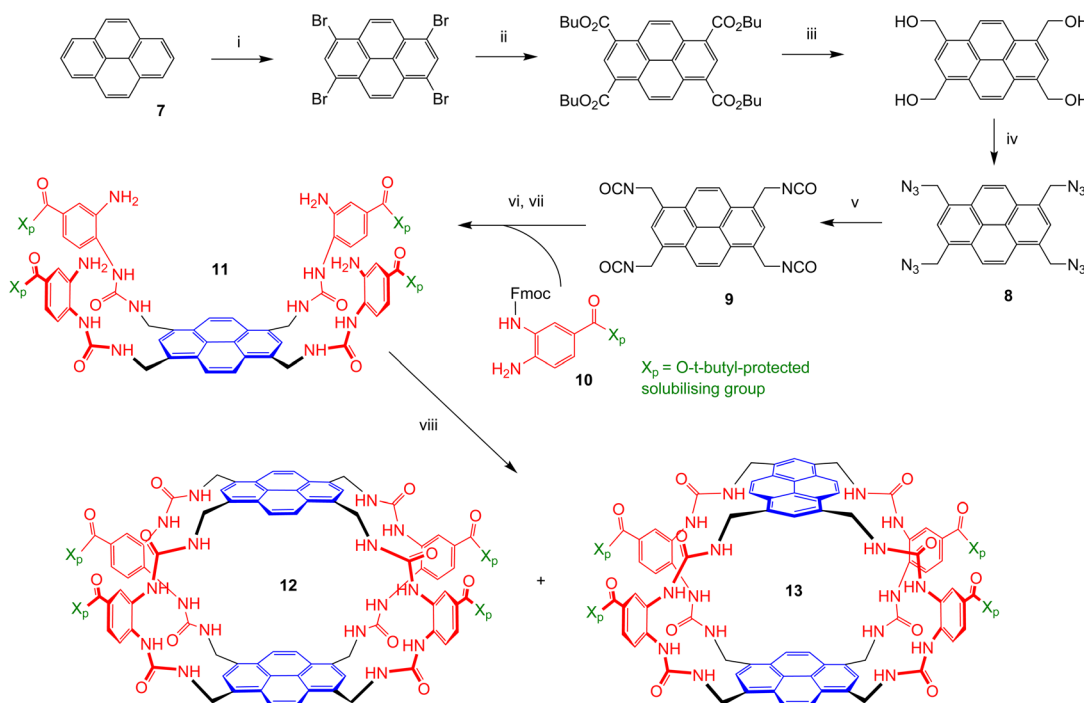
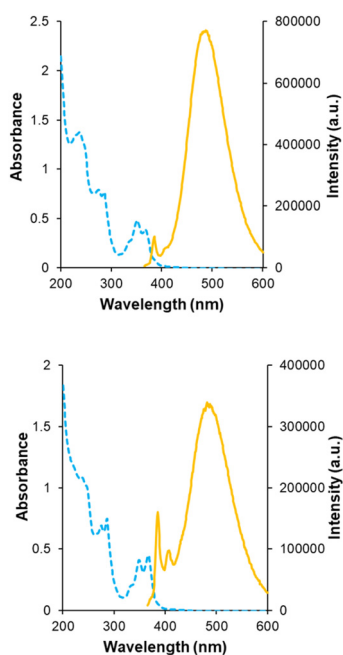


Fig. 2 Second-generation Temples featuring bis-urea spacers. (a) GluHUT **4**, which binds glucose with remarkable strength and selectivity.<sup>6</sup> (b) The pyrene-based receptors reported in this work. For X, see Fig. 1.





**Scheme 1** Synthesis of protected receptors **12** and **13**: (i)  $\text{Br}_2$ ,  $\text{PhNO}_2$ , 98%; (ii)  $\text{BuOH}$ ,  $\text{CO}$  (30 bar), DIPEA,  $\text{Pd}(\text{OAc})_2$ , BINAP, xylenes, 80%; (iii)  $\text{LiBH}_4$ ,  $\text{THF}$ ,  $\text{MeOH}$ , 96%; (iv)  $(\text{PhO})_2\text{PON}_3$ ,  $\text{DMF}$ , DBU, 46%. (v) polymer-supported triphenylphosphine,  $\text{CO}_2$  (20 bar), toluene,  $50\text{ }^\circ\text{C}$ , 95%. (vi) **10**,  $\text{DCM}$ , pyridine, 77%. (vii) DBU,  $\text{DCM}$ , 92%. (viii) **9**,  $\text{DMF}$ ,  $\text{DCM}$ , pyridine, 26% (**12**) and 10% (**13**).



**Fig. 3** Optical measurements for (a) eclipsed receptor **5** and (b) staggered receptor **6** in  $\text{H}_2\text{O}$ . UV-Vis absorbance spectra (blue) at  $12.5\text{ }\mu\text{M}$  and fluorescence emission spectra (orange) at  $0.39\text{ }\mu\text{M}$ , excited at  $340\text{ nm}$ .

than the bis-urea unit in **5** and **6**. The implication is that **2** and **3** maintain open cavities, with pyrene units held apart, while in **5** and **6** the tricyclic structures tend to collapse in water

bringing the pyrenes together. The observation of cavity collapse did not bode well for complex formation, as a substrate would need to prise the surfaces apart. However, in compensation, separating the pyrenes should result in loss of excimer fluorescence providing a reliable and sensitive assay for binding.

Fluorescence titrations were employed to investigate the binding of **5** and **6** to a variety of polar molecules in aqueous phosphate buffer (10 mM, pH 7.4). ESI $\dagger$  was obtained in some cases using  $^1\text{H}$  NMR. Initial dilution studies confirmed that the fluorescence emission from both receptors varied linearly with concentration below  $\sim 2\text{ }\mu\text{M}$ , implying that both were monomeric at least within this concentration range. The strong excimer emission allowed fluorescence titrations to take place at 350 nM receptor concentrations. The substrates are shown in Fig. 4, binding results are summarised in Fig. 4 and Table 1.

For carbohydrate substrates **14–19** no change was observed in fluorescence emission during the titrations, implying that no binding was occurring.  $^1\text{H}$  NMR titrations with glucose **14** and cellobiose **18** in  $\text{D}_2\text{O}$  similarly showed no change in receptor signals. It thus seems that complex formation with carbohydrates does not in general provide sufficient free energy to rearrange either **5** or **6** into a binding conformation. Among aromatic substrates, **20–23** also had no effect on receptor fluorescence, but **24–34** caused significant changes in emission. In all cases the excimer emission decreased, consistent with substrate entering the cavity and separating the pyrene units.<sup>11</sup> For some substrates (“n.d.” in Table 1) the changes were small and roughly linear with concentration, implying a low affinity

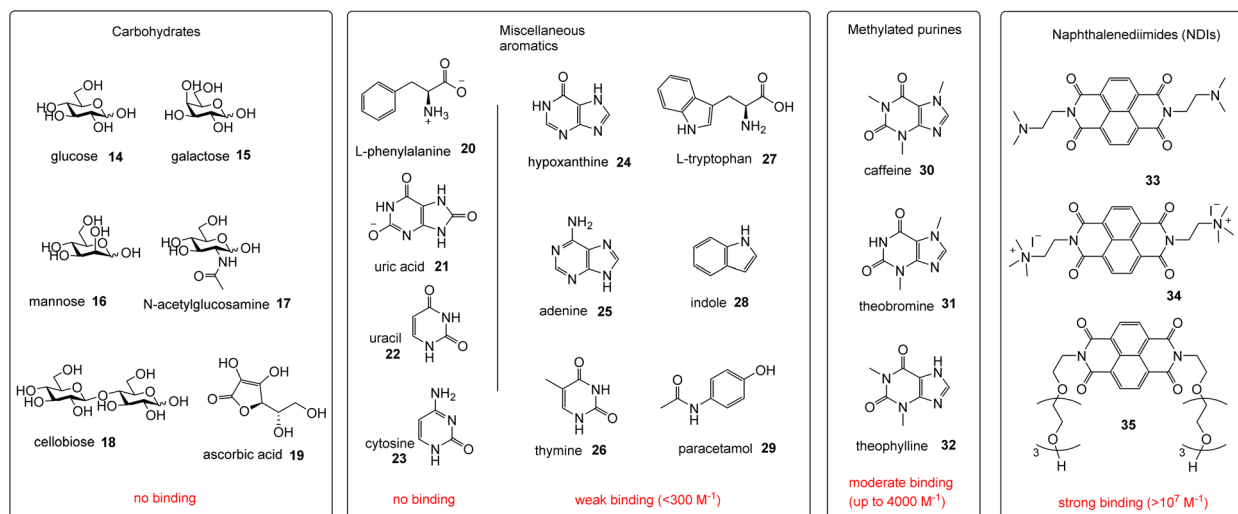


Fig. 4 Substrates for binding studies with receptors 5 and 6 in aqueous phosphate buffer.

Table 1 Binding constants ( $K_a$ ) for aromatic guests to receptors 5 and 6 in aqueous phosphate buffer (10 mM, pH 7.4)

Substrate	Binding constants $K_a$ ( $M^{-1}$ )	
	Eclipsed 5	Staggered 6
Hypoxanthine 24	n.d. <sup>a</sup>	n.d.
Adenine 25	n.d.	288
Thymine 26	n.d.	n.d.
L-Tryptophan 27	61	84
Indole 28	n.d.	n.d.
Paracetamol 29	98	70
Caffeine <sup>b</sup> 30	760	4066
Theobromine <sup>b</sup> 31	1379	3982
Theophylline <sup>b</sup> 32	705	3456
Bis(dimethylamino) <sup>b</sup> NDI 33	$1.6 \times 10^7$	$1.5 \times 10^7$
Bis(trimethylammonium) NDI <sup>b</sup> 34	$2.6 \times 10^7$	$1.7 \times 10^7$

<sup>a</sup> n.d. = not determined; a change in fluorescence emission intensity was observed but was too small for a binding constant to be estimated.

<sup>b</sup> Average of three independent titrations.

that could not be quantified. In other cases the changes were larger, tending towards saturation, and could be fitted to a 1:1 binding isotherm. The resulting binding constants are listed in Table 1. Examples of emission spectra from the titrations are shown in Fig. 5, and binding analysis curves are given in the ESI.†

Notably, among the common aromatic substrates, the methylated purine alkaloids caffeine 30, theobromine 31 and theophylline 32 showed moderately strong binding with affinities in the range ~700–1400 for 5 and ~3500–4000  $M^{-1}$  for 6. In these cases the transition from excimer to pyrene monomer emission was especially clear; see for example Fig. 5a and b. As illustrated in Fig. 6 for receptor 6 + caffeine, the responses to the methylated purines were clearly visible. Visual sensing of these alkaloids, especially caffeine, has attracted much attention,<sup>12</sup> and receptors 5 and 6 may be

added to the options available. The affinities are well-adjusted for estimating [caffeine] in the range observed in real-life samples (~0–5 mM, cf. Fig. 5a). Modelling confirmed that the methylated purines could be good substrates for 5 and 6. As illustrated in Fig. 7 for 5 + caffeine, the carbonyl groups in the substrate can form at least six close interactions to the urea NH groups while the methyl groups lie within the cavity contributing hydrophobic/CH- $\pi$  interactions.

The naphthalenediimide (NDI) fluorophores 33–35 were selected as substrates because they appeared complementary to the cavities of 5 and 6, and seemed likely to bind quite strongly. As illustrated in Fig. 8 for 6 + 34, the four NDI carbonyl groups are positioned to interact well with the bis-urea spacers while the electron-rich pyrene and electron-poor NDI aromatic surfaces should form excellent  $\pi$ - $\pi$ /hydrophobic interactions.<sup>13</sup> Strong binding between synthetic partners is potentially useful in the development of “supramolecular glues”, which can perform roles similar to the much-used avidin/streptavidin-biotin pairings.<sup>14,15</sup> In the event, titrations of both 5 and 6 with all three NDIs caused complete quenching of excimer fluorescence at low substrate concentrations (see e.g. Fig. 5c). Affinities above  $10^7 M^{-1}$  were estimated for all combinations of 5/6 + 33/34. Although much weaker than the (strept)avidin-biotin pairings, for which  $K_a \approx 10^{14} M^{-1}$ , this is within the range considered for “synthavidin” or “noncovalent click” applications<sup>14</sup> and a starting point for further development. The apparent binding constants to 36 were smaller, at  $\sim 10^6 M^{-1}$ , but fluorescence spectra suggested that this NDI was substantially self-associated even at low  $\mu M$  concentrations so that the true values are likely to be higher.  $^1H$  NMR titrations of 5 and 6 with NDIs 34 and 35 resulted in the appearance of new signals consistent with the expected complexes (e.g. Fig. S42 and S44†), implying that complex formation was slow on the  $^1H$  NMR chemical shift timescale. These spectra are discussed further in the following section.



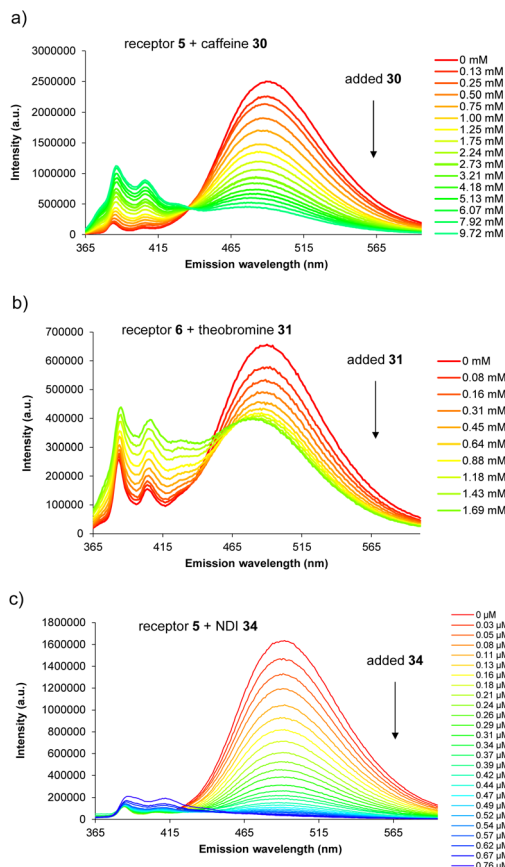


**Fig. 5** Fluorescence spectra from titrations of aromatic substrates into receptors 5 and 6 in 10 mM aqueous phosphate buffer (pH 7.4) at 298 K. (a) Eclipsed receptor 5 (0.35  $\mu$ M) + caffeine 30. (b) Staggered receptor 6 (0.35  $\mu$ M) + theobromine 31. (c) Eclipsed receptor 5 (0.25  $\mu$ M) + naphthalenediimide (NDI) 34.



**Fig. 6** Solutions of receptor 6 with increasing amounts of caffeine 30 under irradiation with UV light.  $\lambda_{\text{ex}} = 365$  nm; [6] = 5  $\mu$ M; solvent = 10 mM aqueous phosphate buffer, [30] (left to right) = 0 mM, 2.5 mM, 5 mM, 10 mM, 20 mM, 40 mM.

### Distinguishing between 5 (eclipsed) and 6 (staggered) connectivities

A key issue in this work was the structural assignment of the two products from cage formation – “eclipsed” structure 12, leading to receptor 5, and “staggered” structure 13 leading to receptor 6. This type of problem has been faced by our group

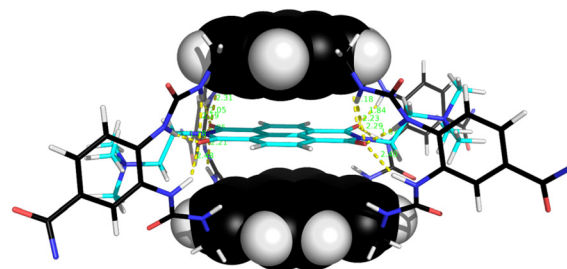


**Fig. 7** Molecular model of receptor 5 binding caffeine 30. The coordinates were obtained from a Monte Carlo Molecular Mechanics (MCMM) conformational search using Maestro–Macromodel, in which the caffeine was allowed to move within the cavity. Energy calculations employed the OPLS3e force field with GB/SA water solvation. Six close NH...OC interactions (1.9–2.5  $\text{\AA}$ ) are shown as yellow broken lines. Receptor side-chains are omitted for clarity.

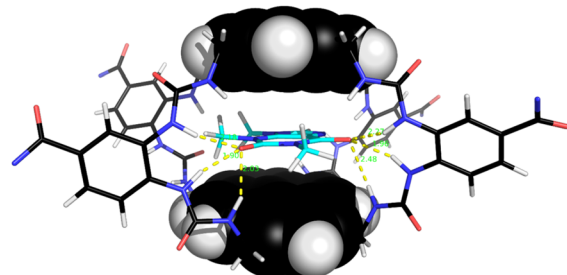


**Fig. 8** Molecular model of receptor 6 binding NDI 34. After minimisation, thirteen NH...OC distances are less than 2.5  $\text{\AA}$  (yellow broken lines). Receptor side-chains are omitted for clarity. Other details as for Fig. 7.

before, in distinguishing between 2 and 3,<sup>4e</sup> and also by Tan, Stoddart and coworkers studying pyrene-based Temples with bis-pyridinium bridges.<sup>16</sup> A particular challenge is that the NMR spectra expected and observed for the two connectivities are closely similar, the only differences being small variations in chemical shifts. Tan, Stoddart & coworkers argued that the p4 protons in their staggered isomer should be shielded by the second pyrene and thus upfield of the corresponding protons in the eclipsed isomer (for proton labelling, see Fig. 9). The p4 protons in their isomers were  $\sim$ 0.1 ppm apart, and the one with the upfield signals was accordingly assigned the staggered connectivity.<sup>16</sup> In the present case, the p4 protons in 12/13, were also  $\sim$ 0.1 ppm apart and the compound with the upfield p4 signals was provisionally assigned staggered structure 13. Fluorescence spectroscopy on 5/6 pointed tentatively in the same direction. The emission spectrum for the compound assigned eclipsed constitution 5 showed a stronger excimer emission and weaker monomer emission than for the compound assigned 6 (Fig. 3, orange traces). This is consistent with greater pyrene-pyrene overlap in a collapsed structure, as might be expected for the eclipsed isomer. The lower binding constants measured for 5 to most substrates (Table 1) support this interpretation, as improved pyrene–pyrene interactions

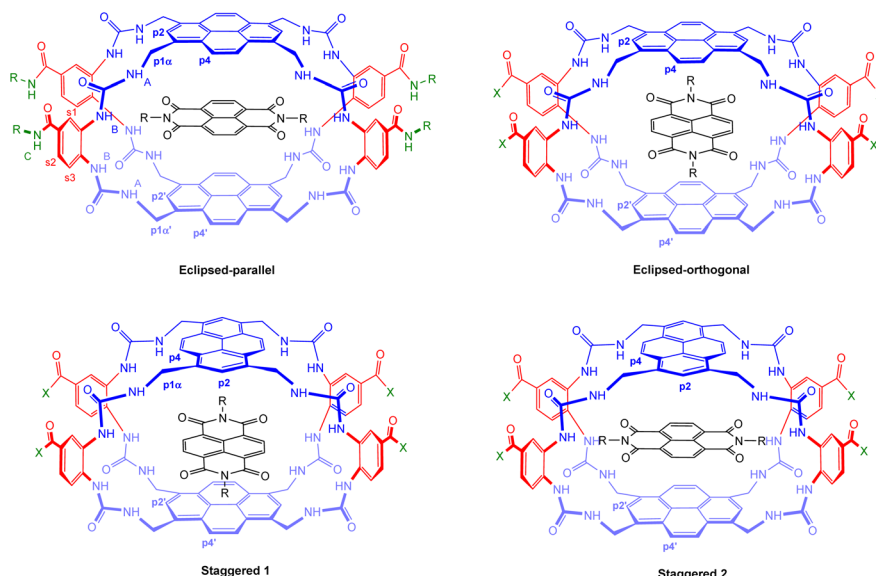


**Fig. 9** Geometries of possible complexes between receptors 5 and 6 and NDIs 33–35. The labelling system used for NMR analysis (Fig. 10) is shown for the eclipsed-parallel arrangement.

would be expected to favour the collapsed cavity and resist opening by a substrate.

To support these assignments, we drew on the  $^1\text{H}$  NMR spectra of the NDI-receptor complexes. It is relevant to note that each receptor can, in principle, form two different complexes with an NDI guest. As illustrated in Fig. 9, the eclipsed isomer 5 can accept the NDI in orientations either parallel or orthogonal to the pyrene units. These are likely to be of substantially different energies, so it is probable that only one will form in practice. In contrast, the staggered isomer 6 can form two complexes which are very similar (**Staggered 1** and **Staggered 2** in Fig. 9). In both cases the NDI is parallel to one pyrene and orthogonal to the other, the only difference being that in **Staggered 1** it is parallel to the pyrene *meta* to COX in the spacer, while in **Staggered 2** it is parallel to the pyrene *para* to COX. These should be similar in energy and one would expect that both would be present in solution.

Detailed NMR analyses were performed on the complexes between the two receptors and NDIs 34 and 35. For the macro-

cycle assigned eclipsed structure 5, the spectra were dominated by a single species in which all receptor protons could be identified *via* 2D methods. The assigned spectrum of 5 + 34 is shown in Fig. 10a. NOESY peaks were observed between NDI side-chain protons and receptor p4 protons, but not the p2 protons. The spectra were thus consistent with the “eclipsed-orthogonal” complex, supporting the eclipsed constitution for the receptor. For the receptor assigned staggered structure 6 paired with NDI 35, a complete set of peaks with NOESY connections could be observed for one complex, but there were also a set of weaker signals suggesting that a second complex was present in the ratio major : minor  $\sim 3 : 1$  (Fig. 10b, starred signals). Following the argument presented above, the evidence for two complexes of similar energy is strongly indicative of the staggered constitution for the receptor. The intermolecular NOEs were difficult to interpret fully, but cross peaks between NDI side-chain protons and both p4 and p2 were also consistent with the staggered receptor structure. Thus fluorescence spectroscopy, NMR of the receptors and

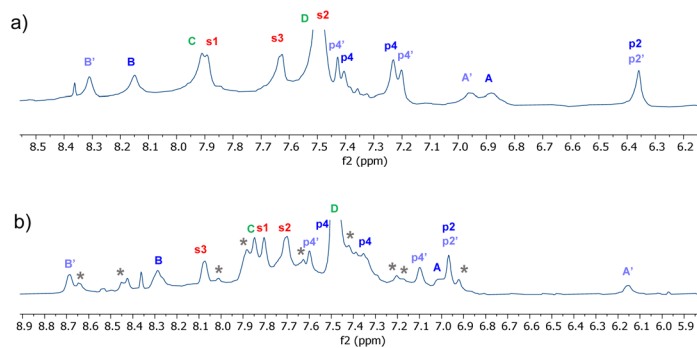


**Fig. 10** Partial  $^1\text{H}$  NMR spectra (700 MHz, 9 : 1  $\text{H}_2\text{O} : \text{D}_2\text{O}$ , 298 K) of (a) Eclipsed receptor 5 (250  $\mu\text{M}$ ) + NDI 34 (750  $\mu\text{M}$ ) and (b) Staggered receptor 6 (250  $\mu\text{M}$ ) + NDI 35 (1 mM). Assignments were made using NOESY correlations, see ESI.† For labelling see Fig. 9, “eclipsed-parallel” combination.



NMR of receptor-NDI complexes all pointed to the assignment shown in this paper.

## Conclusion

In this work, we have shown that the methodology used to prepare bicyclic receptor **GluHUT 4** can be extended to tricyclic octaurea cages **5** and **6**, but that the carbohydrate-binding properties of **4** are not matched by these new structures. We propose that a major reason for the failure to bind saccharides is the collapse of the cavities in **5** and **6**, driven by hydrophobic and  $\pi$ - $\pi$  interactions and signalled by the fluorescence spectra. The contrast between **5/6**, which do not maintain cavities, and the earlier systems **2/3** which do, suggests an important difference between the bis-urea spacer in the second-generation Temples and the isophthalamide pillar which underpins the first. The isophthalamide is relatively rigid and, as far as we can tell, reliable in holding roof and floor apart. The bis-urea is more flexible, and while it presumably holds the triethylbenzene surfaces apart in **4**, it does not succeed with the pyrenes in **5** and **6**. It thus seems the design of second-generation carbohydrate-binding Temples will be more challenging than their earlier cousins, although if conformations can be controlled the binding properties of the bis-urea spacer will hopefully compensate.

Given the collapsed nature of **5** and **6**, it is remarkable that they do show significant binding properties. Purine alkaloids such as caffeine are bound quite strongly, with respectable selectivity, and fluorescence signalling which could be employed in sensing. Napthalenediimides (NDIs) are bound very strongly, to the extent that further development could lead to potential applications in “supramolecular glues”. While other options show higher affinities, the geometrical match between NDI substrate and octaurea cage suggests potential for useful specificity. Host-guest pairs which are orthogonal to each other and can operate simultaneously could allow the development of sophisticated self-assembling systems. The ability to detect binding visually through fluorescence signalling should be advantageous, while the NDI guests could be modified in various ways, potentially increasing affinities.

## Experimental

For detailed experimental procedures see the ESI.†

## Author contributions

APD designed and supervised the project. CSW performed most of the experimental work and interpreted the results. FB prepared the NDI substrates, and assisted with spectroscopic studies. All authors contributed to the writing of the paper.

## Conflicts of interest

There are no conflicts to declare.

## Acknowledgements

We thank the University of Bristol for a studentship to CW, and Dr Christopher Williams for assistance in acquiring 2D NMR spectra.

## References

- (a) H. F. P. Johns, E. E. Harrison, K. J. Stingley and M. L. Waters, Mimicking biological recognition: lessons in binding hydrophilic guests in water, *Chem. – Eur. J.*, 2021, **27**, 6620–6644; (b) L. Escobar and P. Ballester, Molecular recognition in water using macrocyclic synthetic receptors, *Chem. Rev.*, 2021, **121**, 2445–2514; (c) J. Q. Dong and A. P. Davis, Molecular recognition mediated by hydrogen bonding in aqueous media, *Angew. Chem., Int. Ed.*, 2021, **60**, 8035–8048; (d) *Supramolecular Chemistry in Water*, ed. S. Kubik, Wiley-VCH, Weinheim, 2019; (e) P. S. Cremer, A. H. Flood, B. C. Gibb and D. L. Mobley, Collaborative routes to clarifying the murky waters of aqueous supramolecular chemistry, *Nat. Chem.*, 2018, **10**, 8–16; (f) A. P. Davis, S. Kubik and A. D. Cort, Supramolecular chemistry in water, *Org. Biomol. Chem.*, 2015, **13**, 2499–2500; (g) E. A. Kataev and C. Muller, Recent advances in molecular recognition in water: artificial receptors and supramolecular catalysis, *Tetrahedron*, 2014, **70**, 137–167; (h) G. V. Oshovsky, D. N. Reinhoudt and W. Verboom, Supramolecular chemistry in water, *Angew. Chem., Int. Ed.*, 2007, **46**, 2366–2393.
- Selected examples: (a) C. Allott, H. Adams, P. L. Bernad, C. A. Hunter, C. Rotger and J. A. Thomas, Hydrogen-bond recognition of cyclic dipeptides in water, *Chem. Commun.*, 1998, 2449–2450; (b) M. Fokkens, T. Schrader and F. G. Klärner, A molecular tweezer for lysine and arginine, *J. Am. Chem. Soc.*, 2005, **127**, 14415–14421; (c) C. Schmuck, D. Rupprecht and W. Wienand, Sequence-dependent binding of dipeptides by an artificial receptor in water, *Chem. – Eur. J.*, 2006, **12**, 9186–9195; (d) B. Verdejo, G. Gil-Ramirez and P. Ballester, Molecular recognition of pyridine n-oxides in water using calix[4]pyrrole receptors, *J. Am. Chem. Soc.*, 2009, **131**, 3178–3179; (e) E. M. Peck, W. Liu, G. T. Spence, S. K. Shaw, A. P. Davis, H. Destecroix and B. D. Smith, Rapid macrocycle threading by a fluorescent dye-polymer conjugate in water with nanomolar affinity, *J. Am. Chem. Soc.*, 2015, **137**, 8668–8671; (f) A. Lascaux, G. De Leener, L. Fusaro, F. Topic, K. Rissanen, M. Luhmer and I. Jabin, Selective recognition of neutral guests in an aqueous medium by a biomimetic calix 6 cryptamide receptor, *Org. Biomol. Chem.*, 2016, **14**, 738–746; (g) G. B. Huang, S. H. Wang, H. Ke, L. P. Yang and W. Jiang, Selective reco-



gnition of highly hydrophilic molecules in water by endo-functionalized molecular tubes, *J. Am. Chem. Soc.*, 2016, **138**, 14550–14553; (h) H. Yao, H. Ke, X. B. Zhang, S. J. Pan, M. S. Li, L. P. Yang, G. Schreckenbach and W. Jiang, Molecular recognition of hydrophilic molecules in water by combining the hydrophobic effect with hydrogen bonding, *J. Am. Chem. Soc.*, 2018, **140**, 13466–13477; (i) W. Q. Liu, A. Johnson and B. D. Smith, Guest back-folding: a molecular design strategy that produces a deep-red fluorescent host/guest pair with picomolar affinity in water, *J. Am. Chem. Soc.*, 2018, **140**, 3361–3370; (j) O. Francesconi, M. Martinucci, L. Badii, C. Nativi and S. Roelens, A biomimetic synthetic receptor selectively recognising fucose in water, *Chem. – Eur. J.*, 2018, **24**, 6828–6836; (k) G. Peñuelas-Haro and P. Ballester, Efficient hydrogen bonding recognition in water using aryl-extended calix 4 pyrrole receptors, *Chem. Sci.*, 2019, **10**, 2413–2423.

3 (a) A. P. Davis, Synthetic lectins, *Org. Biomol. Chem.*, 2009, **7**, 3629–3638; (b) A. P. Davis, Biomimetic carbohydrate recognition, *Chem. Soc. Rev.*, 2020, **49**, 2531–2545.

4 Examples: (a) E. Klein, M. P. Crump and A. P. Davis, Carbohydrate recognition in water by a tricyclic polyamide receptor, *Angew. Chem., Int. Ed.*, 2005, **44**, 298–302; (b) Y. Ferrand, M. P. Crump and A. P. Davis, A synthetic lectin analog for biomimetic disaccharide recognition, *Science*, 2007, **318**, 619–622; (c) Y. Ferrand, E. Klein, N. P. Barwell, M. P. Crump, J. Jiménez-Barbero, C. Vicent, G. J. Boons, S. Ingale and A. P. Davis, A synthetic lectin for O-linked beta-N-acetylglucosamine, *Angew. Chem., Int. Ed.*, 2009, **48**, 1775–1779; (d) C. Ke, H. Destecroix, M. P. Crump and A. P. Davis, A simple and accessible synthetic lectin for glucose recognition and sensing, *Nat. Chem.*, 2012, **4**, 718–723; (e) P. Rios, T. S. Carter, T. J. Mooibroek, M. P. Crump, M. Lisbjerg, M. Pittelkow, N. T. Supekar, G.-J. Boons and A. P. Davis, Synthetic receptors for the high-affinity recognition of O-GlcNAc derivatives, *Angew. Chem., Int. Ed.*, 2016, **55**, 3387–3392; (f) T. J. Mooibroek, J. M. Casas-Solvas, R. L. Harniman, C. M. Renney, T. S. Carter, M. P. Crump and A. P. Davis, A threading receptor for polysaccharides, *Nat. Chem.*, 2016, **8**, 69–74.

5 D. Van Eker, S. K. Samanta and A. P. Davis, Aqueous recognition of purine and pyrimidine bases by an anthracene-based macrocyclic receptor, *Chem. Commun.*, 2020, **56**, 9268–9271.

6 R. A. Tromans, T. S. Carter, L. Chabanne, M. P. Crump, H. Li, J. V. Matlock, M. G. Orchard and A. P. Davis, A biomimetic receptor for glucose, *Nat. Chem.*, 2019, **11**, 52–56.

7 F. Palacios, C. Alonso, D. Aparicio, G. Rubiales and J. M. de los Santos, The aza-Wittig reaction: an efficient tool for the

construction of carbon-nitrogen double bonds, *Tetrahedron*, 2007, **63**, 523–575.

8 D. Carnaroglio, K. Martina, G. Palmisano, A. Penoni, C. Domini and G. Cravotto, One-pot sequential synthesis of isocyanates and urea derivatives via a microwave-assisted Staudinger-aza-Wittig reaction, *Beilstein J. Org. Chem.*, 2013, **9**, 2378–2386.

9 G. Bains, A. B. Patel and V. Narayanaswami, Pyrene: A probe to study protein conformation and conformational changes, *Molecules*, 2011, **16**, 7909–7935.

10 F. M. Winnik, Photophysics of preassociated pyrenes in aqueous polymer-solutions and in other organized media, *Chem. Rev.*, 1993, **93**, 587–614.

11 Cationic linear and macrocyclic pyrene dimers have shown similar responses to nucleotides. See: Z. Xu, N. J. Singh, J. Lim, J. Pan, H. N. Kim, S. Park, K. S. Kim and J. Yoon, Unique sandwich stacking of pyrene-adenine-pyrene for selective and ratiometric fluorescent sensing of ATP at physiological pH, *J. Am. Chem. Soc.*, 2009, **131**, 15528–15533; A. M. Agafontsev, T. A. Shumilova, A. S. Oshchepkov, F. Hampel and E. A. Kataev, Ratiometric detection of ATP by fluorescent cyclophanes with bellows-type sensing mechanism, *Chem. – Eur. J.*, 2020, **26**, 9991–9997.

12 See for example: O. Francesconi, A. Ienco, C. Nativi and S. Roelens, Effective recognition of caffeine by diaminocarbazolic receptors, *ChemPlusChem*, 2020, **85**, 1369–1373; P. Karmakar, S. Manna, K. Maiti, S. S. Ali, U. N. Guria, R. Sarkar, P. Datta, D. Mandal and A. K. Mahapatra, A perylene diimide based fluorescent probe for caffeine in aqueous medium, *Supramol. Chem.*, 2019, **31**, 28–35; N. Dey, B. Maji and S. Bhattacharya, A versatile probe for caffeine detection in real-life samples via excitation-triggered alteration in the sensing behavior of fluorescent organic nanoaggregates, *Anal. Chem.*, 2018, **90**, 821–829; Z. Kostereli and K. Severin, Array-based sensing of purine derivatives with fluorescent dyes, *Org. Biomol. Chem.*, 2015, **13**, 9231–9235.

13 M. S. Cubberley and B. L. Iverson, <sup>1</sup>H NMR investigation of solvent effects in aromatic stacking interactions, *J. Am. Chem. Soc.*, 2001, **123**, 7560–7563.

14 C. L. Schreiber and B. D. Smith, Molecular conjugation using non-covalent click chemistry, *Nat. Rev. Chem.*, 2019, **3**, 393–400.

15 W. Q. Liu, S. K. Samanta, B. D. Smith and L. Isaacs, Synthetic mimics of biotin/(strept)avidin, *Chem. Soc. Rev.*, 2017, **46**, 2391–2403.

16 W. Liu, Y. Tan, L. O. Jones, B. Song, Q.-H. Guo, L. Zhang, Y. Qiu, Y. Feng, X.-Y. Chen, G. C. Schatz and J. F. Stoddart, PCage: Fluorescent molecular temples for binding sugars in water, *J. Am. Chem. Soc.*, 2021, **143**, 15688–15700.

